Journal of Engineering and Applied Sciences 11 (12): 2697-2702, 2016
ISSN: 1816-949X

Thermal and Mechanical Properties of Polylactic Acid Filled with Organosilane Modified Cellulose Fibril

[1]Sarit Thanomchat and [2]Kawee Srikulkit
[1]Department of Materials Science, Faculty of Science, Chulalongkorn University, 10330 Chulalongkorn, Thailand
[2]Center of Excellent on Petrochemical and Materials Technology, Chulalongkorn University, 10330 Chulalongkorn, Thailand

Abstract: This research was aimed at improving properties of PLA by the addition of Cllulose Fibril (CF) prepared by the dissolution of cotton microcrystalline cellulose in NaOH/urea aqueous system, followed by regeneration of cellulose in an HCl bath. Then, surface hydrophobicity modification of CF was achieved by silanization reaction using hexadecyltrimethoxysilane to obtain Silane-g-CF. Following that, Silane-g-CF/PLA composites with various filler loadings of 0.5, 1.0, 3.0 and 5.0 wt% were prepared by twin screw extrusion and injection molding. The DSC results indicated that Silane-g-CF tended to perform nucleating ability for PLA by lowering the cold crystallization temperature (T_{cc}) as well as inducing the crystallization (T_c) at higher temperature. As consequence, the degree of PLA crystallinity increased in the presence of Silane-g-CF. It was found that Silane-g-CF enhanced the impact resistance of PLA up to 30% arising from the interfacial adhesion as well as compatibility between two phases. In addition, the plasticization effect of silane long alkyl chain resulted in an increase in the percent elongation at break. Unfortunately, the tensile strength and Young's modulus slightly decreased. Finally, SEM micrographs of Silane-g-CF/PLA composites revealed the rougher fracture surface when compared to neat PLA, confirming the better interfacial adhesion and compatibility.

Key words: Cellulose fibril, silanization, polylactic acid, composites, thermal properties, ductility

INTRODUCTION

Polylactic Acid (PLA) is a thermoplastic biopolymer made from the renewable resources such as corn, sugarcane, potato, starch and rice which are fermented into lactic acid (Frone *et al*., 2013). Now a days, PLA has received an attention from both research and industrial fields due to good mechanical properties, biodegradability and easy processing. However, the drawbacks of PLA such as low heat resistance, brittleness, poor crystallization behavior and high cost are still inferior to petroleum-based polymers (Frone *et al*., 2013; Fortunati *et al*., 2010; Lu *et al*., 2014)

Cellulose is the most abundant natural polymer, good mechanical properties, light weight, biodegradability, renewability as well as low cost (Ku *et al*., 2011; Oksman *et al*., 2003). Moreover, it can be used in several forms including film, fibers, microcrystalline cellulose, cellulose nanocrystal, cellulose nanowhisker or microfibrillated cellulose. However, the addition of cellulose into hydrophobic polymers such as PE, PP or PLA exhibits the poor dispersion due to the hydrophilicity of cellulose (Tingaut *et al*., 2009). Therefore, various surface modifications such as silanization, acetylation, grafting or using of a coupling agent are required to improve the dispersibility of cellulose (Abdul Khalil *et al*., 2014; Khalil *et al*., 2012; Kalia *et al*., 2014; Salon *et al*., 2007).

Silanization, one type of surface modifications is commonly employed for modification of cellulose. Under acidic or basic conditions, organosilane, $RSi(OR)_3$, undergoes hydrolysis and condensation reaction with cellulose hydroxyl group, resulting in hydrophobic cellulose. The long alkyl chain (R) on cellulose surface helps improve the compatibility between cellulose and polymer matrix by enhancing the interfacial adhesion between two phases (Frone *et al*., 2013; Bauer *et al*., 2003; Salon *et al*., 2005).

In this study, Cellulose Fibril (CF) prepared by the dissolution/precipitation of cotton microcrystalline cellulose in NaOH/urea system (Thanomchat *et al*., 2014) was hydrophobically modified by organosilane. Modified

Corresponding Author: Kawee Srikulkit, Center of Excellent on Petrochemical and Materials Technology, Chulalongkorn University, 10330 Chulalongkorn, Thailand

CF was used as a filler for PLA. Various contents of modified CF in PLA were investigated using a twin-screw extruder. Thermal properties and mechanical properties of composites were evaluated.

MATERIALS AND METHODS

Experimental: Cellulose Fibril (CF) was prepared according to the previous report ((Thanomchat *et al*., 2014). Cotton microcrystalline cellulose was dissolved in 7 wt% urea/12 wt% NaOH solution at -5°C under continuously stirring until a transparent solution was obtained. The cellulose solution was precipitated in 1.0 M HCl solution and then filtrated and washed with distilled water until the pH value of cellulose gel was approximate to 5. Hexadecyltrimethoxysilane was kindly supplied by Evonik. Nonylphenolethoxylate EO15 (EO15) under the trade name of TERGITOL™ (DOW Chemical Co., Ltd.) was kindly provided by Star Tech Chemical Co., Ltd. DISPERBYK-2008 was purchased from BYK Asia Pacific Pte. Ltd., (Singapore). Commercial grade methanol was bought from a local supplier. About 37% HCl (AR grade, QRëc) was purchased from the local supplier. PLA pellet (2003D grade, Natureworks®) was ordered from BC Polymers Marketing Co., Ltd. Heat stabilizer (Arylphosphite or Alkanox246) was obtained from SCG (Thailand).

Synthesis of organosilane modified cellulose fibril (Silane-g-CF): A 200 g of wet cellulose fibril (equivalent to 10 g of dry CF) was dispersed into 200 m^2 of water and stirred by an overhead stirrer. A mixed solution containing 20 m^2 of 10 %w/v EO15 solution and 5 m^2 of 2.5 %w/v of DISPERBYK2008 was prepared by a homogenizer until a milky solution was obtained, then it was slowly poured into a CF dispersion. The CF dispersion was achieved by a homogenizer. Then, 25 g of hexadecyltrimethoxysilane (HDTMS) was added to the CF dispersion (1: 2.5, CF (based on dried wt): HDTMS wt ratio). After 30 min stirring, 60 mL of methanol was added to the dispersion and continuously stirred for 30 min. Then, concentrated HCl was dropped until the pH value was approximately 2. Once, HCl was added, the viscosity of the mixture increased. The mixture was poured into a tray and left standing at ambient temperature for 2-3 days until dry, obtaining Silane-g-CF (modified CF). Then, Silane-g-CF was subject to freeze/thaw process to obtain Silane-g-CF powder. Silane-g-CF was dried overnight in an oven at 60°C. Finally, Silane-g-CF was sieved through a 100 mesh screen.

Silane-g-CF/PLA composites preparation: A 1 kg of 20 wt% Silane-g-CF/PLA masterbatch was prepared by melt extrusion. Sample preparation was carried out as follows: 10 g of arylphosphite was dissolved in 100 mL toluene followed by an addition of Silane-g-CF (200 g). Then, 800 g of PLA pellet was added to Silane-g-CF dispersion. The mixture was mechanically mixed and then left standing to allow Silane-g-CF precipitation onto PLA surface during toluene evaporation in a fume hood. After toluene was completely evaporated, Silane-g-CF coated PLA pellet was obtained. The sample was put in an oven at 60°C for 24 h prior to melt extrusion. The masterbatch was prepared using a twin-screw extruder (LTE-26-44, Labtech Scientific, Labtech Engineering, Thailand) with a screw diameter of 26 mm and L/D (length/diameter) of 44. The temperature profile from feed zone to die zone was set as 140/150/160/170/170/175/175/175/180/180/180°C, respectively and the screw speed was 30 rpm. The extruded masterbatch was cooled in a water bath and then cut into pellets by a cutting machine (Labtech Scientific, Labtech Engineering, Thailand). The masterbatch was dried in a hopper dryer (SHINI Plastic Technologies) at 60°C.

The PLA composites with the Silane-g-CF contents of 0.5, 1.0, 3.0 and 5.0 wt% were prepared by mixing the calculated amount of masterbatch with virgin PLA pellet. 1.0 wt% of heat stabilizer was added and physically mixed. The mixture was fed into the same twin-screw extruder. The extrusion was conducted using the same condition as masterbatch preparation. The specimens for tensile properties test were molded into a dumbbell-shape by a mini-injection molding machine (HAAKE Mini JetII). The injection temperature was set at 210°C for 5 min. The specimens for impact resistance were also prepared via the injection molding machine (NEX80, Nissei Injection Molding Machine). The temperature profile from feed zone to nozzle was set as 30/190/190/195/195/210°C, respectively.

Characterizations and testing: The impact resistance was measured according to ASTM D256 using an impact testing machine (GT-7045-MD, GOTECH, Taiwan) with a 1.00 J hammer. The tensile properties of samples were determined by a universal testing machine (LR100K, LLOYD, UK) according to ASTM D638. A load cell of 1000 N and crosshead speed of 1 mm min^{-1} were applied. The fractural morphologies of specimens from tensile testing were investigated by a scanning electron microscope (JSM 6460LV, Jeol, Japan) to confirm the effect of Silane-g-CF on the mechanical properties of composites using an acceleration voltage of 15 kV.

The thermal properties of neat PLA and composites were analyzed by a differential scanning calorimeter (DSC1, METTLER TOLEDO, US). The approximate 5 mg

of sample was measured under non-isothermal condition within the temperature range of 25-200°C. The sample was tested by 4 scans including 1st heating, 1st cooling, 2nd heating and 2nd cooling, respectively using the heating rate of 10°C/min and cooling rate of 1°C min^{-1}. To eliminate the previous thermal history, the sample was held at 200°C for 3 min before cooling down. The experiment was carried out under nitrogen flow of 50 mL min^{-1}. The thermal properties such as glass transition temperature (T_g), cold crystallization temperature (T_{cc}), melting temperature (T_m), crystallization temperature (T_c) and enthalpies (ΔH_m, ΔH_{cc} and ΔH_c) were determined from the second heating scan and the second cooling scan. The degree of crystallinity (χ) was calculated as follows:

$$\chi = ((\Delta H_m - \Delta H_{cc})/\Delta H_{m0} \times f)\ 100 \quad (1)$$

Where:

f = The weight fraction of PLA in the composite
Δh_m = The enthalpy of melting
Δh_{cc} = The crystallization enthalpy during the DSC heating scan
Δh_{m0} = The enthalpy of melting for a 100% crystalline PLA taken as 93.0 J/g (Turner *et al*., 2004)

RESULTS AND DISCUSSION

Mechanical properties: Figure 1 shows the impact resistance of all samples. The addition of 0.5, 1.0 and 3.0 wt% Silane-g-CF raises the impact resistance by 10, 20 and 30%, respectively. However, the value slightly begins to drop at 5.0 wt% filler loading due to an agglomeration of filler particles. The improved impact resistance is indicative of the compatibility between filler and matrix. This means that Silane-g-CF plays a role in improving the properties of composite materials (Li and Shimizu, 2009). In this case, the modification of CF by organosilane led to hydrophobic Silane-g-CF which then enhances compatibility as well as interfacial adhesion. As consequence, impact resistance is improved due to the enhancement of toughness (Thepthawat and Srikulkit, 2014). Obviously, the virgin CF fails to improve the brittleness of PLA and the impact resistance dramatically drops approximately by 30%. This result confirms the poorer interfacial adhesion due to the incompatibility between hydrophilic CF and hydrophobic PLA matrix.

The tensile properties are shown in Fig. 2. In comparison with neat PLA, the tensile strength values of Silane-g-CF/PLA composites slightly decrease with an increase in filler content. In similar manner, virgin CF/PLA composite shows similar trend of tensile strength value. Neither Silane-g-CF nor virgin CF improves the modulus of PLA. Fortunately, the elongation at break is found to be higher (5 and 6 % for 0.5 % and 1.0 wt% Silane-g-CF

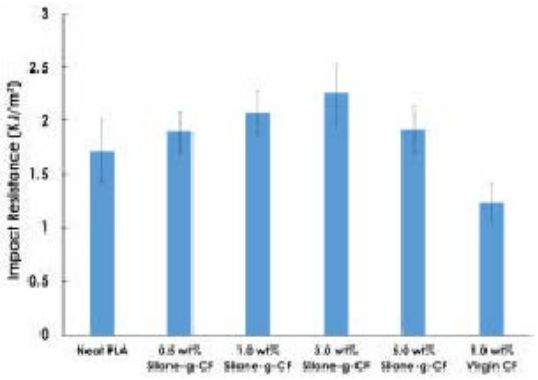

Fig. 1: Impact resistance of neat PLA, Silane-g-CF/PLA composites and virgin CF/PLA composite

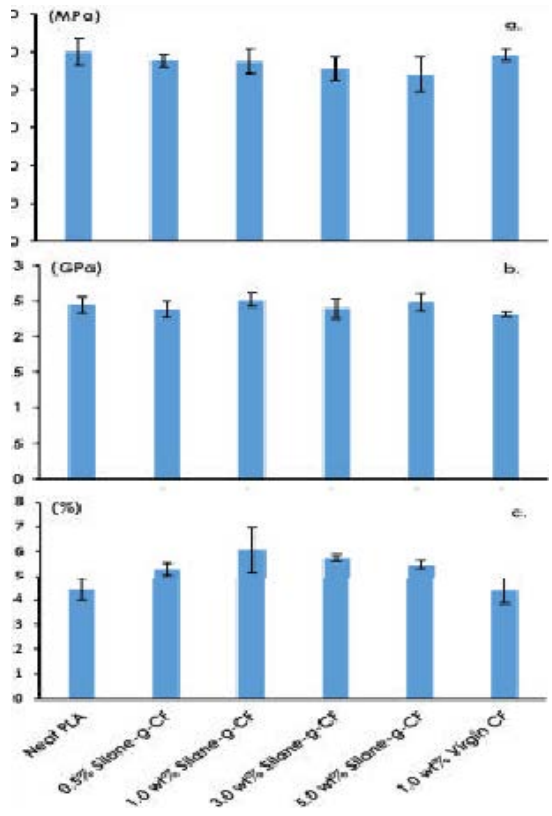

Fig. 2: Impact resistance of neat PLA, Silane-g-CF/PLA composites and virgin CF/PLA composite

loading, respectively). However, the value then slightly drops at 3.0 wt and 5.0 wt% Silane-g-CF loadings. Virgin CF also shows a similar trend. The increase in elongation at break and the decrease in strength and modulus can be explainable based on the effect of plasticizing behavior (Li and Huneault, 2007) arising from the organosilane long alkyl chain on Silane-g-CF. In addition, an increase in

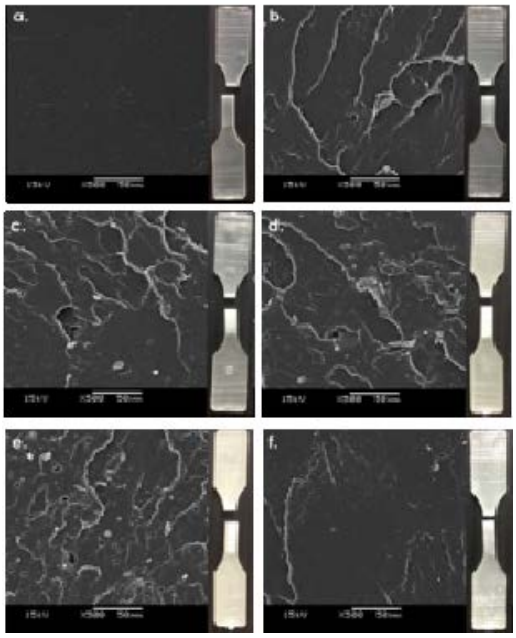

Fig. 3: SEM micrographs of fracture morphology: a) Neat PLA; b) The 0.5 wt% Silane-g-CF; c) The 1.0 wt% Silane-g-CF; d) The 3.0 wt% Silane-g-CF; e) The 5.0 wt% Silane-g-CF; f) The 1.0 wt% of virgin CF

elongation at break implies the enhancing ductility as well as reducing brittleness, resulting in the increasing impact resistance.

The SEM micrographs of fracture surfaces from tensile testing are shown in Fig. 3. The fracture morphology of neat PLA exhibits smoother surface than Silane-g-CF/PLA composites which are rougher, corresponding to higher filler loadings. The rough surface indicates the better interfacial adhesion between filler and matrix, resulting in the increase of elongation at break (Thepthawat and Srikulkit, 2014). The virgin CF/PLA composite also shows the smoother fracture surface compared to Silane-g-CF/PLA composites. The poorer interfacial adhesion as well as incompatibility between virgin CF and PLA fails to improve the percent elongation at break. Moreover, impact resistance is found to decrease notably. The significant deformation of Silane-g-CF/PLA composites indicates that Silane-g-CF is capable of absorbing energy, resulting in the improved impact resistance (Lu *et al*., 2014). However, the agglomeration of Silane-g-CF can be observed at 3.0 and 5.0 wt% loadings, resulting in adverse effect of high filler loadings on mechanical properties.

Thermal properties: The DSC heating thermograms of PLA and composites at heating rate of 10°C/min (Fig. 4a) show T_g, T_{cc} and T_m which are typical characteristics of a semi-crystalline polymer (Suryanegara *et al*., 2010). In this case, the steric effect of filler particles obstructs an orientation of PLA molecular chains, leading to an increase of polymer matrix free volume. As a result, T_g is found to decrease in this case (Krishnamachari *et al*., 2009; Lee *et al*., 2003).

Both 0.5 and 1.0 wt% Silane-g-CF/PLA composites show the lower cold crystallization temperature (T_{cc}) when compared to neat PLA. In addition, an absence of T_{cc} is observed at higher filler loading. These results indicate that Silane-g-CF can induce the faster crystallization and enhance the crystallinity by acting as a nucleating agent. Silane-g-CF promotes heterogeneous nucleation mechanism which induces a decrease in free energy barrier and triggers crystallization (Kang *et al*., 2008). In comparison with Silane-g-CF, virgin CF also exhibits decreasing T_{cc} which the peak intensity still exists in 2nd heating endotherm, attributing to the poor self-nucleation of PLA.

The two melting peaks are observed in all cases. It is known that PLA crystals have a large tendency to reorganize into more stable structures via continuous partial melting-recrystallization-perfection mechanism during heating scan (Lorenzo, 2006). Therefore, the reorganization of small or imperfect crystals from the previous cooling leads to a multiple melting behavior which is related to T_{m1} (the melting of less perfect crystalline structure) while T_{m2} is attributed to the more perfect crystalline structure (Frone *et al*., 2013). Neat PLA shows the lower melting peak (T_{m1}) at 147.5°C and the higher melting peak (T_{m2}) at 155.7°C. However, T_{m1} of composites shifts to a lower temperature while T_{m2} remains unchanged. The shift of T_{m1} is associated with the decrease of T_{cc} which is caused by the restriction of chain segment mobility. The decrease in chain mobility leads to the smaller lamellae, resulting in lower melting temperature. However, when the primary lamellae melts, the recrystallization of chain segments can occur at almost the same temperature to form the new lamellae with similar thickness. Therefore, all composites exhibit the similar T_{m2} (Lu *et al*., 2014).

Figure 4b presents the crystallization peak (T_c) of neat PLA and composites obtained from 2nd cooling scan. The small crystallization peak of neat PLA is observed at 95.6°C while T_c of Silane-g-CF/PLA composites shifts to higher temperature due to the nucleation effect. In case of virgin CF, the addition of virgin CF into PLA suppresses T_c to 94°C, indicating its poorer nucleating performance when compared to Silane-g-CF. Therefore, the results confirm that Silane-g-CF performs the good nucleating

Table 1: Thermal properties obtained from second heating and second cooling scan

Filler loading	T_g /°C	T_{cc}/°C	Δh_{cc}/Jg^{-1}	T_{m1}/°C	T_{m2}/°C	Δh_m/Jg^{-1}	T_c/°C	ΔH_c/Jg^{-1}	χ/%
Neat PLA	56.0	112.1	22.6	147.5	155.7	34.8	95.6	18.0	13.1
0.5 wt% Silane-g-CF	54.3	105.3	6.0	144.8	154.8	38.7	96.7	38.1	35.3
1.0 wt% Silane-g-CF	54.5	107.2	6.6	145.1	154.8	37.3	97.1	38.6	33.3
3.0 wt % Silane-g-CF	55.0	-	-	144.6	154.8	35.4	98.7	38.7	39.2
5.0 wt% Silane-g-CF	53.7	-	-	145.0	155.0	37.0	100.7	38.2	41.9
1.0 wt% virgin CF	54.3	105.5	17.1	145.7	155.0	37.8	94.2	33.0	22.5

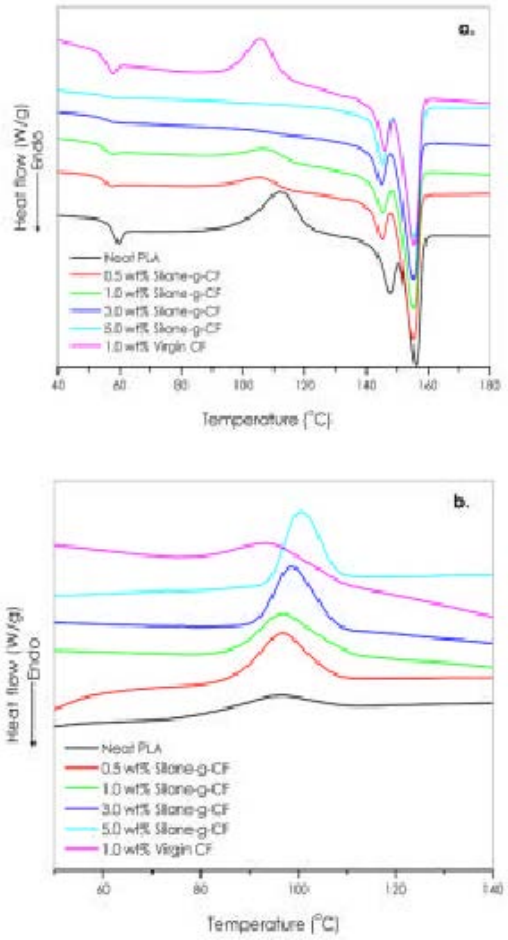

Fig. 4: DSC thermograms of neat PLA and composites: a) Second heating; b) Second cooling

ability for PLA. The addition of Silane-g-CF enhances the degree of crystallinity up to 20-29% depending on filler content whereas virgin CF just slightly increases the degree of crystallinity around 9%. The experiment data are summarized in Table 1.

CONCLUSION

Cellulose Fibril (CF), prepared by dissolution of cotton microcrystalline cellulose in NaOH/urea system, followed by cellulose precipitation in an HCl bath was employed as a filler for PLA. To enhance the compatibility with PLA, the CF surface was successfully modified via silanization using hexadecyltrimethoxysilane as a modifying agent. Combination of two surfactants was employed to achieve the fully modified CF. As a result, improved properties of PLA loaded with Silane-g-CF were evident. An increase in the impact resistance and elongation at break was related to the good interfacial adhesion as well as compatibility between Silane-g-CF and PLA which was evidenced by the presence of rougher surface of fractured composites. However, the plasticization effect generated by the organosilane long alkyl chain caused the decrease of tensile strength and Young's modulus. It could be concluded that Silane-g-CF played a dominant role in nucleating PLA judged by the lower cold crystallization temperature and the higher crystallization temperature, resulting in an increase in the degree of crystallinity.

ACKNOWLEDGEMENTS

The researchers would like to thank The 90th Anniversary of Chulalongkorn University (Ratchadaphiseksomphot Endowment Fund GCUGR 1125582011D) and the Royal Golden Jubilee Ph.D. Program (PHD/0182/2553) for the financial support of this research.

REFERENCES

Abdul Khalil, H.P.S., Y. Davoudpour, M.N. Islam, A. Mustapha, K. Sudesh, R. Dungani and M. Jawaid, 2014. Production and modification of nanofibrillated cellulose using various mechanical processes: A review. Carbohydr. Polym., 99: 649-665.

Bauer, F., H.J. Glasel, U. Decker, H. Ernst and A. Freyer *et al.*, 2003. Trialkoxysilane grafting onto nanoparticles for the preparation of clear coat polyacrylate systems with excellent scratch performance. Progress Organic Coatings, 47: 147-153.

Fortunati, E., I. Armentano, A. Iannoni and J.M. Kenny, 2010. Development and thermal behaviour of ternary PLA matrix composites. Survey Ophthalmol., 55: 2200-2206.

Frone, A.N., S. Berlioz, J.F. Chailan and D.M. Panaitescu, 2013. Morphology and thermal properties of PLA-cellulose nanofibers composites. Carbohydr. Polym., 91: 377-384.

Kalia, S., S. Boufi, A. Celli and S. Kango, 2014. Nanofibrillated cellulose: Surface modification and potential applications. Colloid Polym. Sci., 292: 5-31.

Kang, K.S., S.I. Lee, T.J. Lee, R. Narayan and B.Y. Shin, 2008. Effect of biobased and biodegradable nucleating agent on the isothermal crystallization of poly (lactic acid). Korean J. Chem. Eng., 25: 599-608.

Khalil, H.A., A.H. Bhat and A.I. Yusra, 2012. Green composites from sustainable cellulose nanofibrils: A review. Carbohydr. Polym., 87: 963-979.

Krishnamachari, P., J. Zhang, J. Lou, J. Yan and L. Uitenham, 2009. Biodegradable poly (lactic acid)-clay nanocomposites by melt intercalation: A study of morphological, thermal and mechanical properties. Int. J. Polym. Anal. Charact., 14: 336-350.

Ku, H., H. Wang, N. Pattarachaiyakoop and M. Trada, 2011. A review on the tensile properties of natural fiber reinforced polymer composites. Composit. Eng., 42: 856-873.

Lee, J.H., T.G. Park, H.S. Park, D.S. Lee and Y.K. Lee *et al*., 2003. Thermal and mechanical characteristics of poly (L-lactic acid) nanocomposite scaffold. Biomater., 24: 2773-2778.

Li, H. and M.A. Huneault, 2007. Effect of nucleation and plasticization on the crystallization of poly (lactic acid). Polym., 48: 6855-6866.

Li, Y. and H. Shimizu, 2009. Improvement in toughness of poly (l-lactide)(PLLA) through reactive blending with acrylonitrile-butadiene-styrene copolymer (ABS): Morphology and properties. Eur. Polym. J., 45: 738-746.

Lorenzo, M.L.D., 2006. Calorimetric analysis of the multiple melting behavior of poly (L-lactic acid). J. Appl. Polym. Sci., 100: 3145-3151.

Lu, T., M. Jiang, X. Xu, S. Zhang and D. Hui *et al*., 2014. The effects on mechanical properties and crystallization of poly (l-lactic acid) reinforced by cellulosic fibers with different scales. J. Appl. Polym. Sci., 131: 1-18.

Oksman, K., M. Skrifvars and J.F. Selin, 2003. Natural fibres as reinforcement in polylactic acid (PLA) composites. Compos. Sci. Technol., 63: 1317-1324.

Salon, M.C.B., G. Gerbaud, M. Abdelmouleh, C. Bruzzese and S. Boufi *et al*., 2007. Studies of interactions between silane coupling agents and cellulose fibers with liquid and solid-state NMR. Magn. Reson. Chem., 45: 473-483.

Salon, M.C.B., M. Abdelmouleh, S. Boufi, M.N. Belgacem and A. Gandini, 2005. Silane adsorption onto cellulose fibers: Hydrolysis and condensation reactions. J. Colloid Interface Sci., 289: 249-261.

Suryanegara, L., A.N. Nakagaito and H. Yano, 2010. Thermo-mechanical properties of microfibrillated cellulose-reinforced partially crystallized PLA composites. Cellul., 17: 771-778.

Thanomchat, S., K. Srikulkit, B. Suksut and A.K. Schlarb, 2014. Morphology and crystallization of polypropylene-microfibrillated cellulose composites. Kmutnb Int. J. Appl. Sci. Technol., 7: 23-34.

Thepthawat, A. and K. Srikulkit, 2014. Improving the properties of polylactic acid by blending with low molecular weight polylactic acid-g-natural rubber. Polym. Eng. Sci., 54: 2770-2776.

Tingaut, P., T. Zimmermann and L.F. Suevos, 2009. Synthesis and characterization of bionanocomposites with tunable properties from poly (lactic acid) and acetylated microfibrillated cellulose. Bio macromolecules, 11: 454-464.

Turner, J.F.I.I., A. Riga, A. O'connor, J. Zhang and J. Collis, 2004. Characterization of drawn and undrawn poly-L-lactide films by differential scanning calorimetry. J. Therm. Anal. Calorim., 75: 257-268.